Supplementary Information for

Precession cycles of the El Niño/Southern Oscillation-like system controlled by Pacific upper-ocean stratification

Shuai Zhang[1,2], Zhoufei Yu[3], Xun Gong[4,5,6], Yue Wang[7], Fengming Chang[2,6*], Gerrit Lohmman[5], Yiquan Qi[1] and Tiegang Li[6,8*]

[1] *Hohai University, Nanjing 210098, China.*
[2] *Key Laboratory of Marine Geology and Environment, Institute of Oceanology, Chinese Academy of Sciences, Qingdao 266071, China.*
[3] *Nanjing Institute of Geology and Palaeontology, Chinese Academy of Sciences, Nanjing 210008, China.*
[4] *Hubei Key Laboratory of Marine Geological Resources, China University of Geosciences, Wuhan 430074, China.*
[5] *Alfred Wegener Institute, Helmholtz Centre for Polar and Marine Research, Bussestrasse. 24, 27570 Bremerhaven, Germany.*
[6] *Qingdao National Laboratory for Marine Science and Technology, Qingdao, 266237, China.*
[7] *State Key Laboratory of Marine Geology, Tongji University, Shanghai, 200092, China.*
[8] *Key Laboratory of Marine Sedimentology and Environmental Geology, First Institute of Oceanography, MNR, Qingdao 266061, China.*

This PDF file includes:

Supplementary Figures 1 to 11
Supplementary text 1: Foraminiferal Mg/Ca measurement
Supplementary text 2: Assessment of the dissolution effect
Supplementary References

* *Correspondence to:* chfm@qdio.ac.cn

* *Correspondence to:* tgli@fio.org.cn

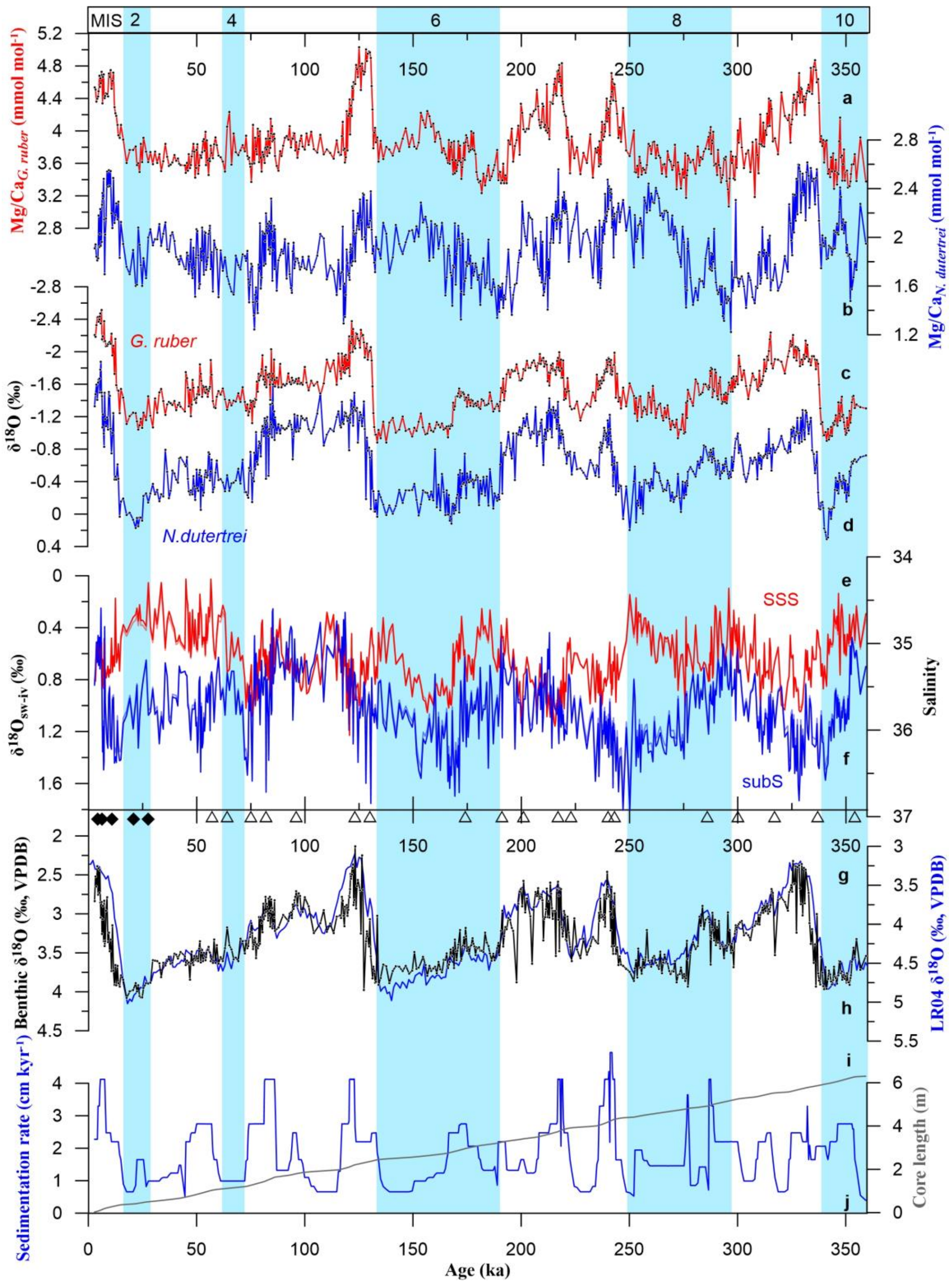

Supplementary Fig. 1 Foraminifera records from core KX97322-4. (a) Mg/Ca values of *G. ruber*; (b) Mg/Ca values of *N. dutertrei*; (c) $\delta^{18}O$ values of *G. ruber*; (d) $\delta^{18}O$ values of *N. dutertrei*; (e) $\delta^{18}O_{sw\text{-}iv}$ and sea surface salinity calculated from *G. ruber*; (f) $\delta^{18}O_{sw\text{-}iv}$ and subsurface water salinity calculated from *N. dutertrei*; (g) $\delta^{18}O$ values of benthic foraminifer *C. wuellerstorfi*; (h) the LR04 benthic stack[1]; (i) core length; (j) sedimentation rate of core KX97322-4. Five AMS ^{14}C ages (black diamonds) and 21 benthic foraminiferal tie points (white triangles) are marked on the X-axis.

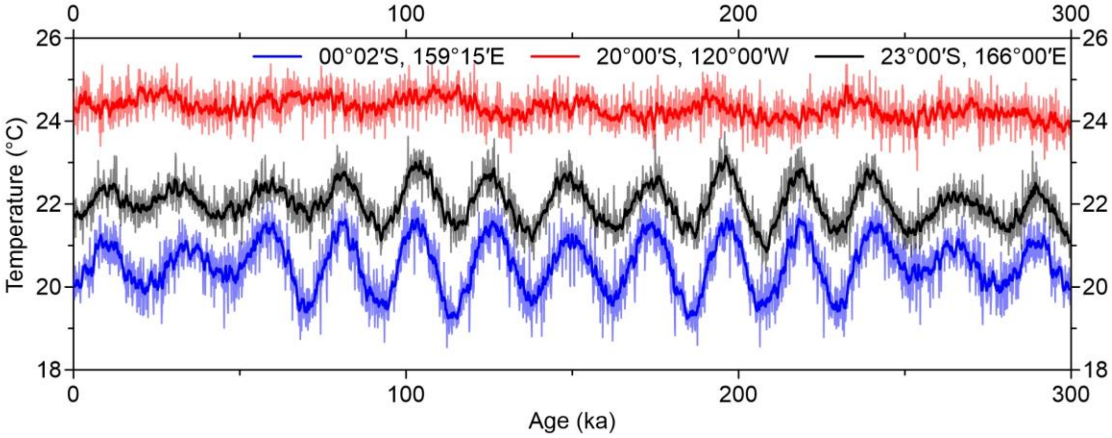

Supplementary Fig. 2 Comparison of simulated subT (blue) at 150 m water depth in October at our core location with simulated SSTs of the subduction zones in the southeastern Pacific (20°00′S, 120°00′E, red) and southwestern Pacific (23°00′S, 166°00′W, black).

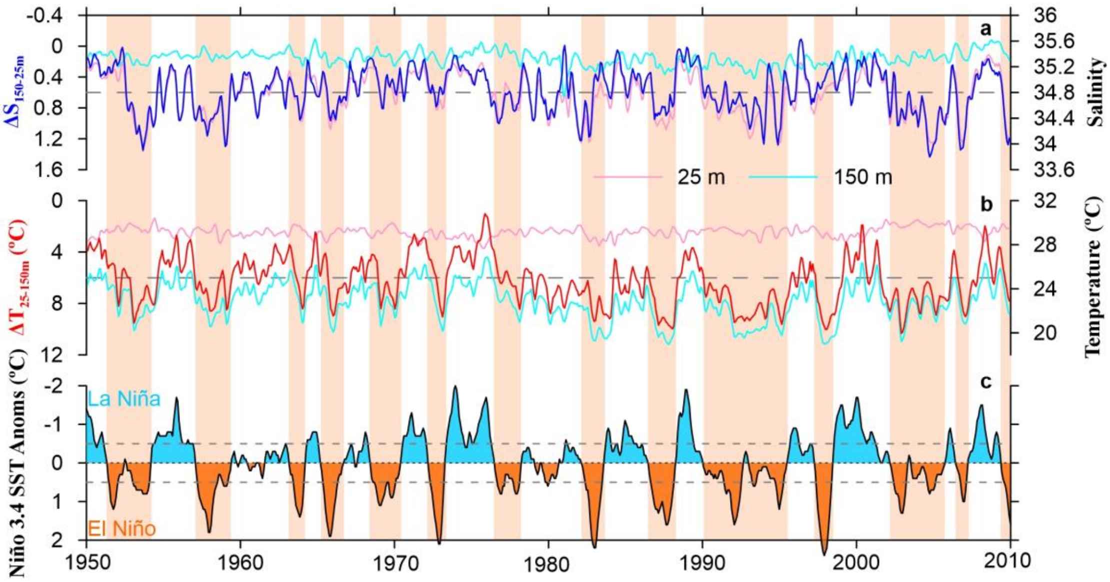

Supplementary Fig. 3 Comparison of the modern observed vertical salinity (a) and temperature (b) differences between 25 m and 150 m water depths at site KX97322-4 with Niño 3.4 SST anomalies from 1950 to 2010 (c). The pink and cyan lines indicate salinity (a) and temperature (b) data at 25 and 150 m, respectively. Orange bars indicate El Niño intervals. Seawater salinity and temperature data come from the Simple Ocean Data Assimilation (SODA) reanalysis dataset (v2.2.4, http://apdrc.soest.hawaii.edu/datadoc/soda_2.2.4.php). The Niño 3.4 index is the 3-month running means of ERSST.v4 SST anomalies in the Niño 3.4 region (http://www.cpc.ncep.noaa.gov).

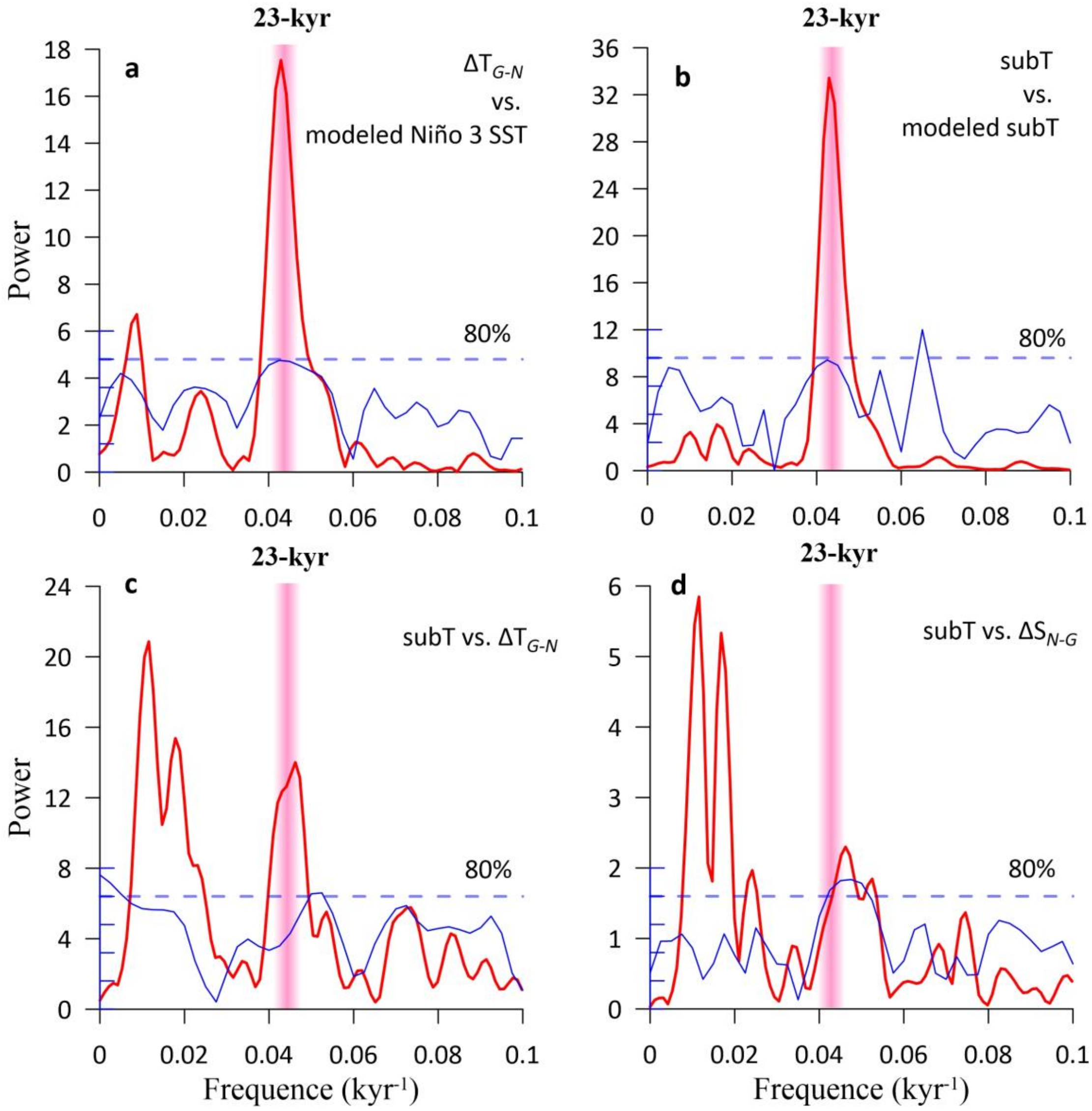

Supplementary Fig. 4 Cross-spectrum analysis of the 500-year smoothed proxies. (a) $\Delta T_{G\text{-}N}$ vs. modeled Niño 3 SST, **(b)** subT vs. modeled subT, **(c)** subT vs. GIG-detrended vertical $\Delta T_{G\text{-}N}$ and **(d)** subT vs. $\Delta S_{N\text{-}G}$. The red curves are cross-spectrum results, and the blue curves are coherency-spectrum results with the dashed curves representing their confidence levels. Shaded bars represent the 23-kyr signals.

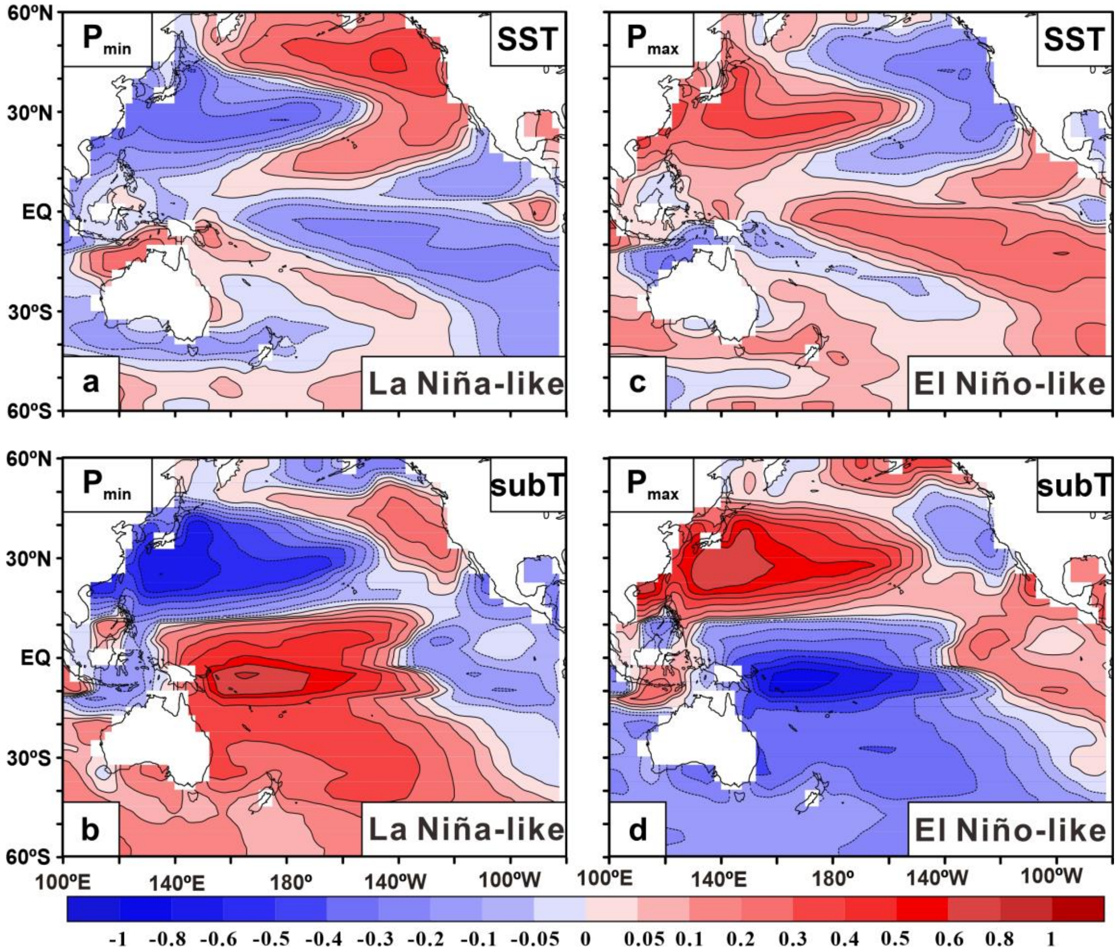

Supplementary Fig. 5 Composite differences (°C) of SST and subT during P_{min} (a and b) and P_{max} (c and d) relative to the 300-kyr climatological mean from the CESM simulation.

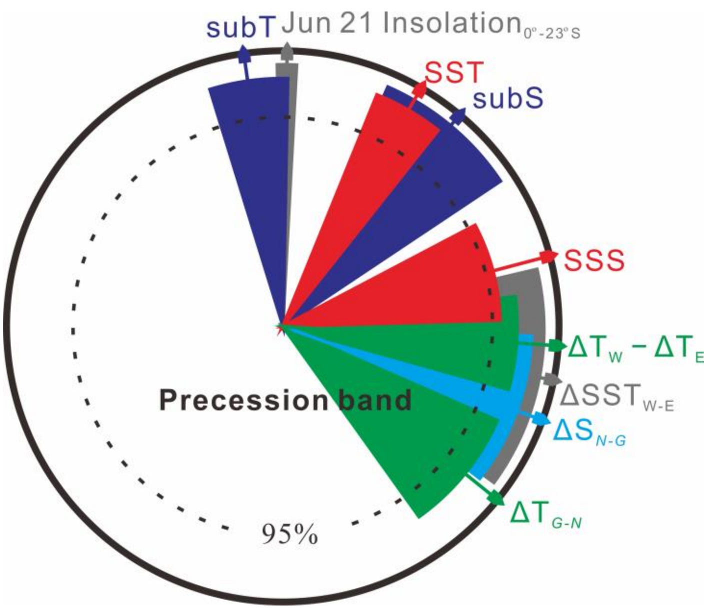

Supplementary Fig. 6 Phase wheels for records of temperature and salinity in the upper water column in the equatorial Pacific. The precession parameter minimum is the black circle at the 12 o'clock position (0). In the precession bandwidth, the subT maximum of site KX97322-4 (−8.1 ± 9.1°) is almost in phase with the precession minimum and the maximum value of the insolation difference between 0° and 23°S on June 21 (0.9 ± 2.1°), leading SST (30.1 ± 8.1°), subS (39.8 ± 16.3°), SSS (75.2 ± 13.1°), the difference in thermocline depth (94.1 ± 11.5°) and ΔSST (101.3 ± 24.7°) between the WEP and EEP, $\Delta S_{N\text{-}G}$ (109.9 ± 17.7°) and $\Delta T_{G\text{-}N}$ (129.0 ± 15.4°). The confidence levels are at least 95%, with the exception of ΔSST, which is 90%.

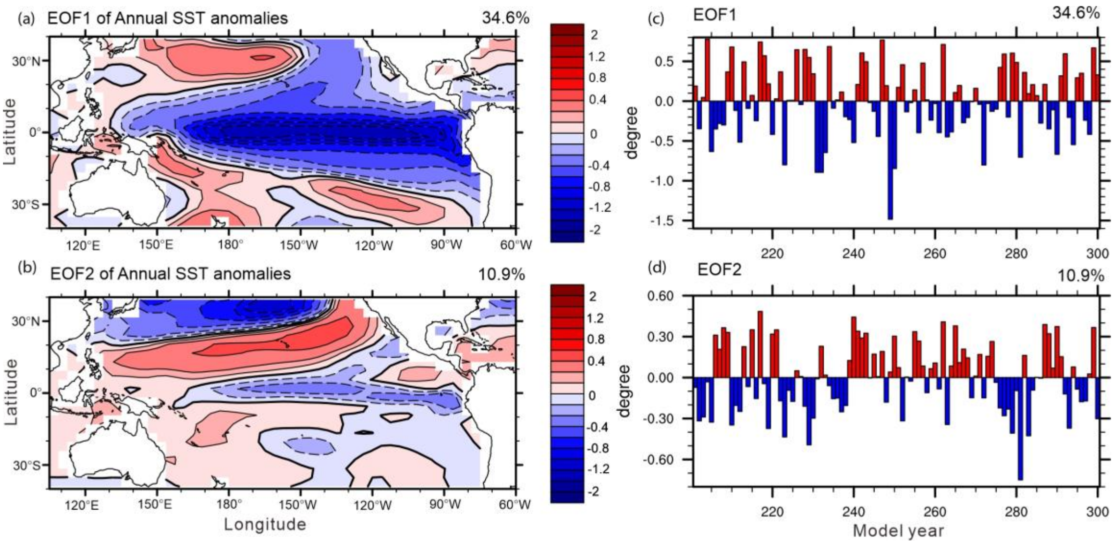

Supplementary Fig. 7 EOFs for annual SST anomalies in the tropical Pacific from the CESM modern control experiment (201–300 years). PC1 and PC2 spatial distributions are displayed on the left (a and b), while PC1 and PC2 time series are shown on the right (c and d). The top right values indicate each EOF's contribution to the total variance.

Foraminiferal Mg/Ca measurement

Fe/Ca, Al/Ca and Mn/Ca analyses were performed to monitor contamination by clays or Mn carbonates. The ranges of Fe/Ca, Al/Ca and Mn/Ca in our samples are 0–0.45, 0–0.93 and 0–0.27 mmol mol^{-1}, respectively (Supplementary Fig. 8), with no correlation with the Mg/Ca ratio (Supplementary Fig. 9), indicating that the samples were not contaminated.

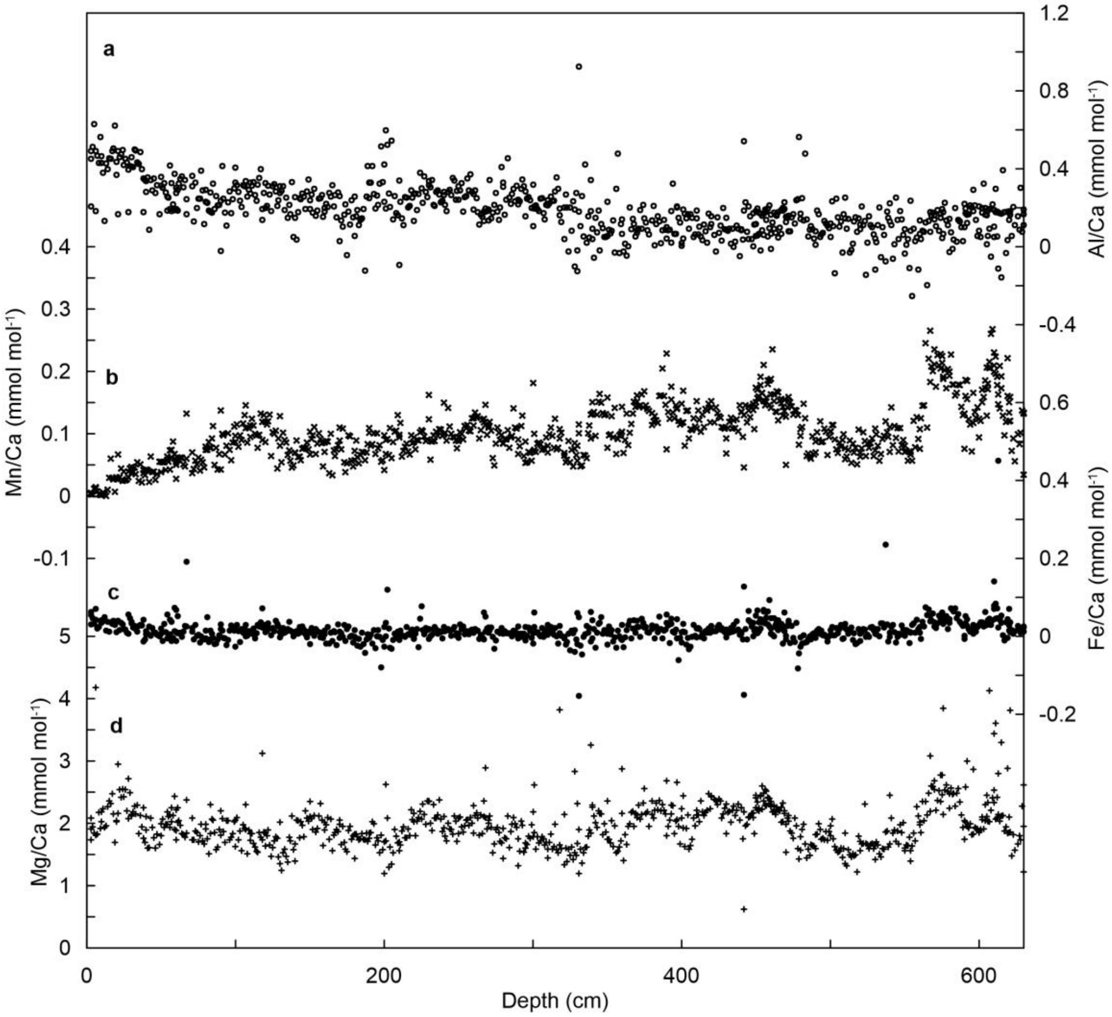

Supplementary Fig. 8 Trace element variations in the tests of *N. dutertrei* in core KX97322-4 with core depth: **(a)** Al/Ca, **(b)** Mn/Ca, **(c)** Fe/Ca and **(d)** Mg/Ca.

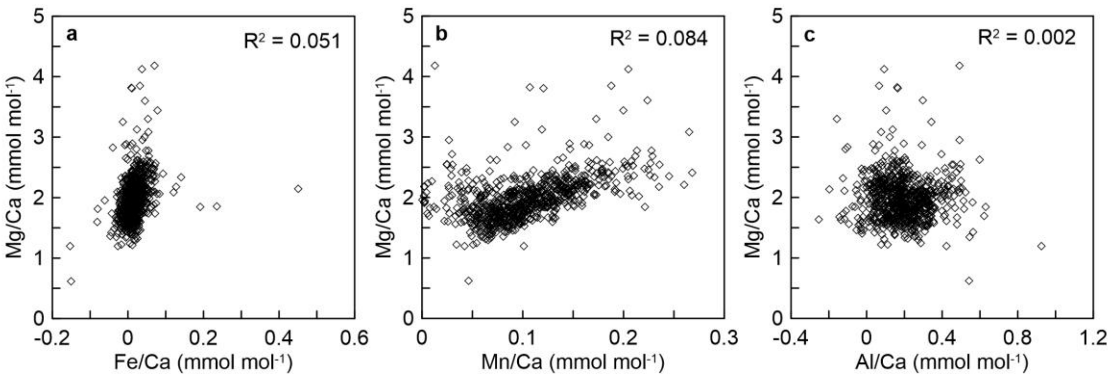

Supplementary Fig. 9 Geochemical ratio plots of KX97322-4 *N. dutertrei*: **(a)** Mg/Ca vs. Fe/Ca, **(b)** Mg/Ca vs. Mn/Ca and **(c)** Mg/Ca vs. Al/Ca.

Assessment of the dissolution effect

Previous work has emphasized an intense bottom water dissolution effect over the Ontong Java Plateau (OJP), reflected by the decreased carbonate ion concentration ($[CO_3^{2-}]$) in the deep sea[2-5]. It would influence the measured Mg/Ca ratios through differential dissolution and mask the actual signal[3]. The size-normalized weight (SNW) of the planktonic foraminiferal test can reflect the variation in the seawater carbonate system and is applied to correct the foraminiferal Mg/Ca thermometer[4,5]. Thus, we tried to correct our Mg/Ca ratios by foraminiferal test weight since the last interglacial period.

Fifty *G. ruber* tests (250–300 μm) and *N. dutertrei* tests (300–355 μm) were picked from each sample to calculate the SNW. Picked foraminiferal tests were subjected to sonication (50 kHz) with ultrapure water, alcohol, and H_2O_2 for 2 s and then sonicated with 2% sodium hexametaphosphate solution for 4 s[4]. After cleaning, we weighed the remaining intact tests in an aluminum boat (12 × 4 × 2.6 mm) on a Sartorius SE2 ultramicro balance with 0.1 μg resolution. Then, the minimum circumscribed circle diameter of the foraminiferal test was measured with ZEN 2.5 software (Carl Zeiss) as the foraminiferal test size. The SNW for each sample was calculated by normalizing the test weight to the corresponding standard diameter:

$$\text{SNW} = \frac{W}{\sum_{i=1}^{n} D_i} \times D_{standard} \quad (1)$$

where W is the total test weight of a sample, D_i is the diameter of each individual test in the sample and $D_{standard}$ is the mean test diameter of the specimens in all samples of this study.

The results show that the SNW of *G. ruber* ranges from 6.58 to 9.85 μg and that of *N. dutertrei* ranges from 18.28 to 24.46 μg. First, by comparing the SNW results with foraminiferal Mg/Ca values and deep water [CO_3^{2-}] over the OJP reconstructed from the B/Ca ratio of the benthic foraminifer *Cibicidoides wuellerstorfi*[2], no correlations were found among them for the last glacial cycle (Supplementary Fig. 10a and Fig. 11a, b, d, e). Second, we used the equations with correction terms for the dissolution effect to correct the Mg/Ca thermometer:

$$\text{Mg/Ca (mmol mol}^{-1}) = (0.025 \times \text{SNW} (\mu g) + 0.11) \exp [0.095 \times \text{SST} (°C)] \quad (2)$$ [5]

and

$$\text{Mg/Ca (mmol mol}^{-1}) = 0.33 \exp 0.09 \times [\text{SST} (°C) + 0.042(\text{SNW} (\mu g) - 12.6)/0.22] \quad (3)$$ [3,6]

for *G. ruber* and

$$\text{Mg/Ca (mmol mol}^{-1}) = 0.28 \exp 0.07 \times [\text{subT} (°C) + 0.165(\text{SNW} (\mu g) - 19.19)/0.62] \quad (4)$$ [3,7]

for *N. dutertrei*. The corrected Mg/Ca temperatures show no discernible difference from the uncorrected temperatures (Supplementary Fig. 10b and 11c, f). Moreover, the corrected subT is abnormally high (Supplementary Fig. 10b), which deviates from the modern observations (Supplementary Fig. 2b). In addition, previous works have reported that the foraminiferal lysocline on the OJP is between 3400[8] and 3600 m[9,10]. During the last 800 kyr, the variation in the lysocline in the equatorial Pacific has obvious glacial-interglacial cycles with an amplitude of 400-800 m[11]; as a result, its influence on our location (2362 m) is limited. As a result, given the small changes in the subT and ΔT data after the correction, we chose not to apply the dissolution correction to our Mg/Ca data in this study.

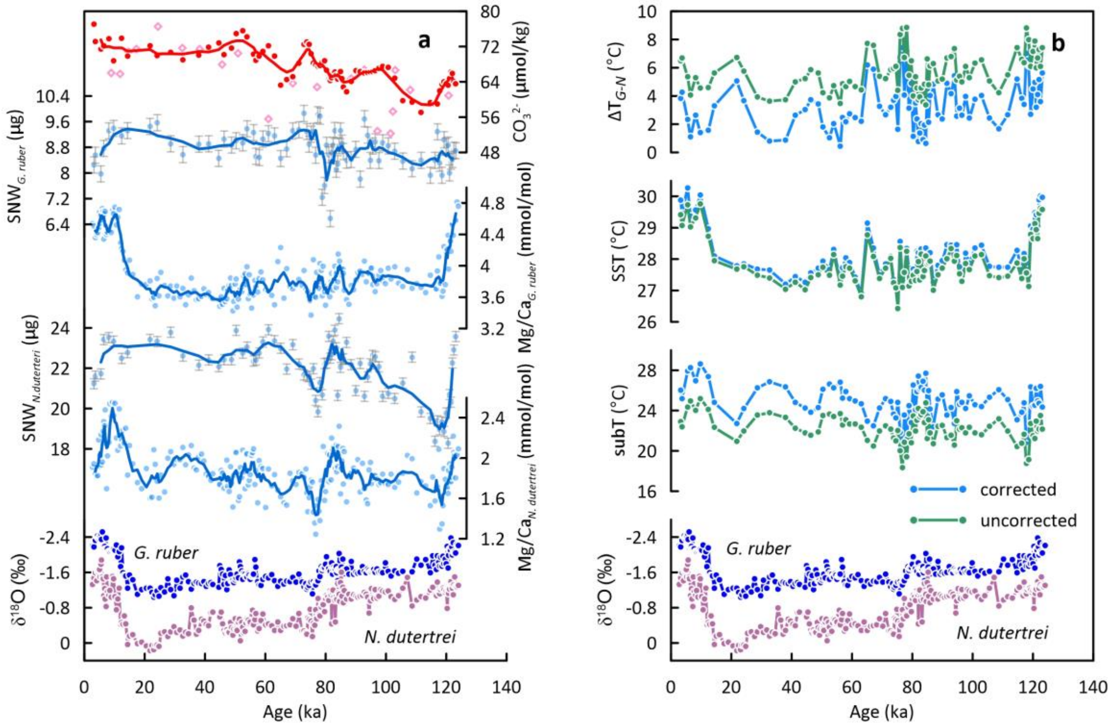

Supplementary Fig. 10 Variations in (a) size-normalized weight (SNW) of *G. ruber* and *N. dutertrei*, as well as (b) SNW-corrected Mg/Ca temperatures in core KX97322-4 since the last interglacial period. The red deep sea [CO_3^{2-}] data were reconstructed on the Ontong Java Plateau[2]. The error bars in (a) are errors of replication (±0.25μg).

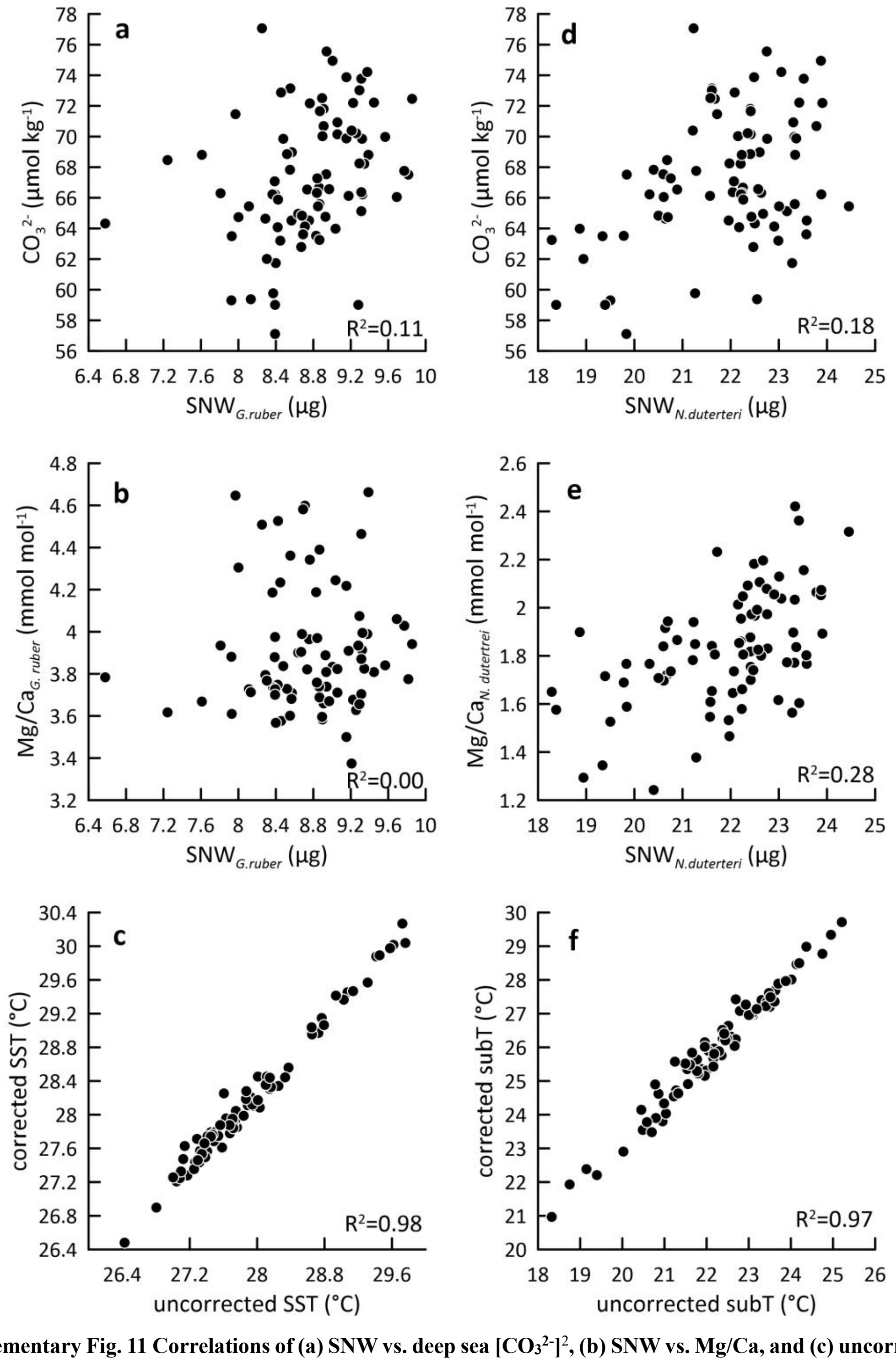

Supplementary Fig. 11 Correlations of (a) SNW vs. deep sea [CO_3^{2-}]^2, (b) SNW vs. Mg/Ca, and (c) uncorrected SST vs. corrected SST from *G. ruber*, and correlations of (d) SNW vs. deep sea [CO_3^{2-}], (e) SNW vs. Mg/Ca, and (f) uncorrected subT vs. corrected subT from *N. dutertrei*.

Supplementary References

1 Lisiecki, L. E. & Raymo, M. E. A Pliocene-Pleistocene stack of 57 globally distributed benthic δ18O records. *Paleoceanography* **20**, PA1003 (2005).

2 Yu, J. *et al.* Responses of the deep ocean carbonate system to carbon reorganization

during the Last Glacial–interglacial cycle. *Quat. Sci. Rev.* **76**, 39-52 (2013).

3 Dekens, P. S., Lea, D. W., Pak, D. K. & Spero, H. J. Core top calibration of Mg/Ca in tropical foraminifera: Refining paleotemperature estimation. *Geochem. Geophys. Geosyst.* **3**, 1-29 (2002).

4 Qin, B., Li, T., Xiong, Z., Algeo, T. J. & Chang, F. Deepwater carbonate ion concentrations in the western tropical Pacific since 250 ka: Evidence for oceanic carbon storage and global climate influence. *Paleoceanography* **32**, 351-370 (2017).

5 Rosenthal, Y. & Lohmann, G. P. Accurate estimation of sea surface temperatures using dissolution-corrected calibrations for Mg/Ca paleothermometry. *Paleoceanography* **17**, 1044 (2002).

6 de Villiers, S. Foraminiferal shell-weight evidence for sedimentary calcite dissolution above the lysocline. *Deep Sea Res., Part I* **52**, 671-680 (2005).

7 Broecker, W. & Clark, E. An evaluation of Lohmann's foraminifera weight dissolution index. *Paleoceanography* **16**, 531-534 (2001).

8 Berger, W., Bonneau, M. & Parker, F. Foraminifera on the deep-sea floor-lysocline and dissolution rate. *Oceanologica Acta* **5**, 249-258 (1982).

9 Wu, G., Yasuda, M. K. & Berger, W. H. Late Pleistocene carbonate stratigraphy on Ontong-Java Plateau in the western equatorial Pacific. *Marine Geology* **99**, 135-150 (1991).

10 Wu, G. & Berger, W. H. Pleistocene δ18O records from Ontong-Java Plateau: Effects of winnowing and dissolution. *Marine Geology* **96**, 193-209 (1991).

11 Farrell, J. W. & Prell, W. L. Climatic change and CaCO3 preservation: An 800,000 year bathymetric Reconstruction from the central equatorial Pacific Ocean. *Paleoceanography* **4**, 447-466 (1989).